Journal of Chromatography A, 1218 (2011) 4117–4125

Contents lists available at ScienceDirect

Journal of Chromatography A

journal homepage: www.elsevier.com/locate/chroma

On the no-field method for void time determination in flow field-flow fractionation

Michel Martin*, Mauricio Hoyos

Ecole Supérieure de Physique et de Chimie Industrielles, Laboratoire de Physique et Mécanique des Milieux Hétérogènes (PMMH – UMR 7636 CNRS – ESPCI ParisTech – Université Pierre et Marie Curie – Université Paris-Diderot), 10 rue Vauquelin, 75231 Paris Cedex 05, France

ARTICLE INFO

Article history:
Available online 12 January 2011

Keywords:
Flow field-flow fractionation
Void time
Void volume
No-field method
Flow profile
Pressure profile
Unretained analytes

ABSTRACT

Elution time measurements of colloidal particles injected in a symmetrical flow field-flow fractionation (flow FFF) system when the inlet and outlet cross-flow connections are closed have been performed. This no-field method has been proposed earlier for void time (and void volume) determination in flow FFF Giddings et al. (1977) [8]. The elution times observed were much larger than expected on the basis of the channel geometrical volume and the flow rate. In order to explain these discrepancies, a flow model allowing the carrier liquid to flow through the porous walls toward the reservoirs located behind the porous elements and along these reservoirs was developed. The ratio between the observed elution time and expected one is found to depend only on a parameter which is a function of the effective permeability and thickness of the porous elements and of the channel thickness and length. The permeabilities of the frits used in the system were measured. Their values lead to predicted elution times in reasonable agreement with experimental ones, taking into account likely membrane protrusion inside the channel on system assembly. They comfort the basic feature of the flow model, in the no-field case. The carrier liquid mostly bypasses the channel to flow along the system mainly in the reservoir. It flows through the porous walls toward the reservoirs near channel inlet and again through the porous walls from the reservoirs to the channel near channel outlet before exiting the system. In order to estimate the extent of this bypassing process, it is desirable that the hydrodynamic characteristics of the permeable elements (permeability and thickness) are provided by flow FFF manufacturers. The model applies to symmetrical as well as asymmetrical flow FFF systems.

1. Introduction

In the Brownian retention mode of field-flow fractionation (FFF), sample components (or analytes) are separated according to their degree of interaction with the external field applied through the channel. They are thus separated according to the force, F, exerted by the external field on a molecule (or particle) of an analyte, in a direction perpendicular to that of the flow of carrier liquid. This force displaces the analyte molecules toward one of the channel walls (the accumulation wall), and the analyte becomes non-uniformly distributed in the direction of the field. This analyte is advected in the longitudinal direction of the channel by the flow of the carrier liquid. If the flow velocity profile was uniform (as it is the case for an electroosmotic flow in an electro-driven system, except in the very thin region near the channel walls), two differently distributed analytes would be advected at the same velocity and no separation would result. If the carrier velocity profile is itself non-uniform, for instance, when it has the parabolic profile characteristic of a pressure-driven laminar flow, the mean migration velocities (advection velocities) of two differently distributed analytes are, most likely, different. Then, the interaction of an analyte with the applied force field is reflected through its advection velocity or, more generally, through its retention ratio, R, which is the ratio of its advection velocity to the cross-sectional average carrier flow velocity [1]. For straight channels, these velocities are rectilinear velocities, while, for azimuthal flow in curved channels, such as those of sedimentation FFF, R should strictly be a ratio of angular velocities [2]. By means of an appropriate retention model, the retention ratio, R, is related to the force F exerted by the field on the analyte molecules. This allows to characterize the analyte as well as to optimize the separation of analytes undergoing different field forces [3].

Being a velocity ratio, R, can generally not be directly measured. It has to be derived from other observable and measurable quantities, such as the mean residence time, or retention time, t_R, of the analyte, and the void time, t_o, which is the elution time of an unretained analyte, i.e. an analyte which does not interact with the applied field and which is, therefore, uniformly distributed within

* Corresponding author. Tel.: +33 140794707; fax: +33 140794523.
E-mail address: martin@pmmh.espci.fr (M. Martin).

0021-9673/$ – see front matter © 2011 Elsevier B.V. All rights reserved.
doi:10.1016/j.chroma.2011.01.010

the carrier liquid, and travels along the channel at the average velocity of the carrier liquid. Indeed, when a constant field is applied along a straight channel of length L, the analyte advection velocity, $\mathcal{V}$, is equal to L/t_R, while the advection velocity of an unretained analyte migrating at the mean flow rectilinear velocity, $\langle v \rangle$, is equal to L/t_o. Hence, one gets:

$$R \equiv \frac{\mathcal{V}}{\langle v \rangle} = \frac{t_o}{t_R} \tag{1}$$

Alternatively, the volumes, V_R and V_o, of carrier effluent flowing from the channel outlet during times t_R and t_o, and called retention volume and void volume, respectively, can be measured. If F_o is the carrier flow rate measured at the channel outlet, these volumes are, respectively, equal to $F_o t_R$ and $F_o t_o$. Hence R can alternatively be obtained as:

$$R = \frac{V_o}{V_R} \tag{2}$$

An accurate characterization of the analyte requires an accurate determination of R, hence an accurate measurement of both t_R and t_o (or of V_R and V_o). The determination of the retention time of an analyte is directly linked to the analysis of this analyte and t_R is obtained as the first temporal moment of the signal provided by a concentration-sensitive flow-through detector connected to the channel outlet during the analysis of the analyte.

The determination of t_o is not as straightforward as that of t_R, because a detectable unretained analyte is not always present in the sample to be analyzed or because it cannot always be ascertained that a given analyte with a low molar mass is effectively unretained even if the large diffusivity of small molecular compounds tends to favor their uniform distribution in the field direction. In fact, for a 250 μm thick channel operated at 20 °C, it can be shown that the force induced by the field on a molecule or particle of the void time probe must not exceed 1.3×10^{-17} N or 0.4×10^{-17} N when the tolerated relative error on t_o is 1% or 0.1%, respectively. When determining t_o with a low molar mass species in the flow and field conditions used for the analysis of the sample, these conditions are easily fulfilled in sedimentation FFF. In thermal FFF, with typical values of the Soret coefficient of low molar mass probes (about 0.01 K^{-1}), these conditions can be satisfied if the temperature difference across the channel does not exceed about 75 K and 25 K, for tolerated errors on t_o of 1% and 0.1%, respectively. But then, complications arising from carrier density stratification occurring in the cross-section due to the applied temperature gradient must be taken into account for the proper definition of t_o [4].

In flow FFF, with typical values of the diffusion coefficient of low molar mass compounds (about 10^{-9} m^2/s), the cross-flow velocity should not exceed 3.1 or 1.0 μm/s for tolerated errors on t_o of 1% and 0.1%, respectively. These values are relatively low and would not allow a sufficient retention for samples with components having moderate molar masses (i.e. for instance, proteins molar masses smaller than about 30,000 or 1,000,000 for tolerated errors on t_o of 1% and 0.1%, respectively) or particle sizes (smaller than about 6 and 18 nm, for t_o tolerated errors of 1% and 0.1%, respectively). Hence, the injection of a low molar mass compound as a t_o probe in conditions optimized for the analysis of such samples would result in significant errors on t_o. If it is, in principle, allowed in conditions used for analyzing components of relatively large sizes, its use was found difficult because these t_o probes can be lost through membranes [5]. Nevertheless, the measurement of the elution time of a small species (copper sulfate) was made in an asymmetrical flow FFF channel on the fraction of the sample that did not wash out of the channel through the accumulation wall [5].

Since, as noted above, t_o should be equal to $L/\langle v \rangle$, and since the mean flow velocity is equal to the ratio, F_o/S_c, of the axial flow rate and the cross-sectional area of the channel, S_c, t_o should become equal to:

$$t_o = \frac{LS_c}{F_o} = \frac{V_g}{F_o} \tag{3}$$

where V_g is equal to the geometrical volume of the channel. Hence, the unretained elution volume, V_o, is equal to V_g. The determination of t_o by means of Eq. (3) using the measured flow rate F_o and the geometrical channel volume calculated from the values, known from construction, of the channel thickness, breadth and length has been used in the FFF literature, especially in sedimentation FFF. In thermal FFF, as mentioned above, such a determination must be modified to take into account the thermal expansion of the carrier in the channel [4]. In flow FFF, it has been noted that membrane protrusion in the channel space may occur on channel assembly [6,7], which hence modifies the channel volume. The method based on geometrical volume calculation may thus be inaccurate in flow FFF.

To ensure that void time probes are really unretained in flow FFF, it was suggested to perform the measurement in absence of cross-flow [8]. In such conditions, both small and relatively large compounds are unretained. This approach was used in early flow FFF studies [6,8]. However, the possibility of partitioning of the void time or void volume probe into the stagnant pore space of the frit making the depletion wall, thus leading to erroneous results was mentioned [9].

In the present study, we further investigate this no-field method for void time determination in flow FFF, when the inlet and outlet cross-flow connections are closed. Doing this, we recognize, that behind the frit making the depletion wall and the other frit backing the semi-permeable membrane of the accumulation wall, are present reservoirs (also called compartments or chambers) for repartition of the cross-flow on the depletion side and collection of the permeate on the accumulation side. Although they are rarely evoked in flow FFF publications and their geometrical characteristics are not mentioned, these compartments are, in practice, present in most flow FFF and asymmetrical flow FFF channels [10–14]. We consider that the carrier liquid contained in the porous frits may not be stagnant, but may flow to and from the reservoirs. The objective is to study the influence of such transverse flow on the void time determination.

2. Theory

We first consider the case of a single porous wall, which corresponds to the situation encountered in asymmetrical flow FFF, then the case of two porous walls corresponding to flow FFF (or symmetrical flow FFF).

2.1. A single porous wall

The system considered in this case is depicted in Fig. 1A and consists of a channel of length L, thickness w and breadth b (assumed constant all along the channel). One wall is solid (bottom wall in Fig. 1A), the second wall is permeable and consists of a porous element (e.g., a frit) of height h, having a permeability k. The length and breadth of this element are assumed equal to those of the channel. The sealing is assumed to be perfect, so that there is no possibility of leak along the porous element edges. Behind the porous element is the reservoir.

The following assumptions are made:

(1) there is no axial flow within the porous element. The flow through the porous element is thus assumed perpendicular to the main channel axis, which amounts to assume that, in the porous element, the axial pressure gradient is small compared

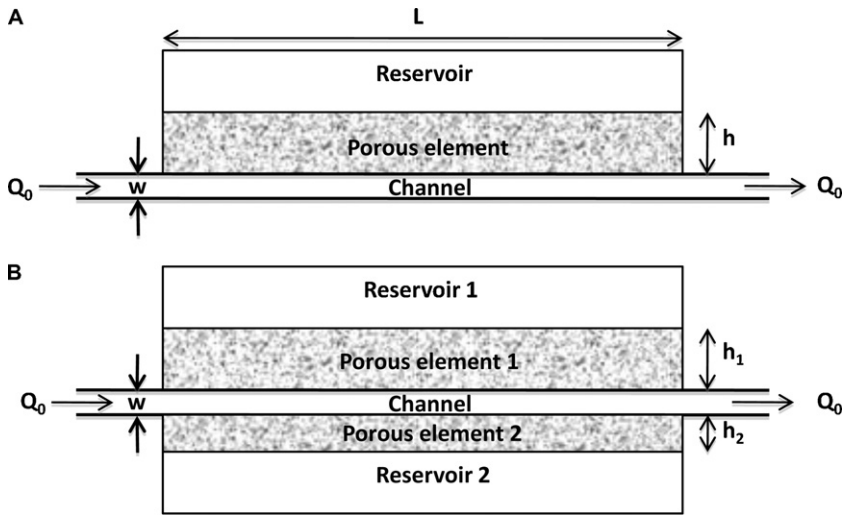

Fig. 1. Schematic diagram of the system assembly considered in the model: (A) asymmetrical flow FFF channel with a single porous wall; (B) symmetrical flow FFF channel with two porous walls.

to the transversal pressure gradient, because essentially h is significantly smaller than L;

(2) the pressure in the reservoir is uniform and equal to P_r. In fact, there is an apparent contradiction when stating that P_r is constant (hence that the pressure gradient along the reservoir is 0) and that there is possibility of axial flow in the reservoir (since the average flow velocity in the reservoir is proportional to the axial pressure gradient in the reservoir). This assumption amounts to state that the pressure difference along the reservoir is negligible compared with the difference between the pressure P_i at the channel inlet and the pressure P_o at the channel outlet. Hence, if w_r and b_r are the heights and breadths of the reservoir, $(w^3 b)/(w_r{}^3 b_r)$ is well smaller than 1. For practical purposes, this condition is fulfilled in present-day asymmetrical flow FFF instruments.

In the following, the flow rates are noted Q. But because we consider a 2-D problem, they have dimension, not of volume per unit time, but of volume per unit channel breadth, b, per unit time (i.e. $Q_{ax} = F_{ax}/b$). Subscripts "c" and "r" describe channel and reservoir quantities, respectively. z is the distance along the channel, from channel inlet ($0 \le z \le L$).

2.1.1. Flow in an infinitesimal slice of the system, at position z

Let us consider an infinitesimal slice of length dz of the whole system assembly. In the channel itself, one has, according to Poiseuille law:

$$Q_{ax,c}(z) = -\frac{w^3}{12\eta}\frac{dP_c}{dz} \tag{4}$$

since the channel permeability is $w^2/12$ (infinite parallel plate configuration) and the cross-section is $w \times 1$ (since one considers flow rate per unit channel breadth). $P_c(z)$ is the pressure in the channel at position z, η is the dynamic viscosity of the carrier liquid. The subscript "ax" describes axial flow.

In steady state conditions, there is no liquid accumulation in the considered slice. Hence the total flow rate entering the slice equals the total flow rate leaving the slice. Since axial flow occurs only in the channel and in the reservoir (not, according to hypothesis 1, in

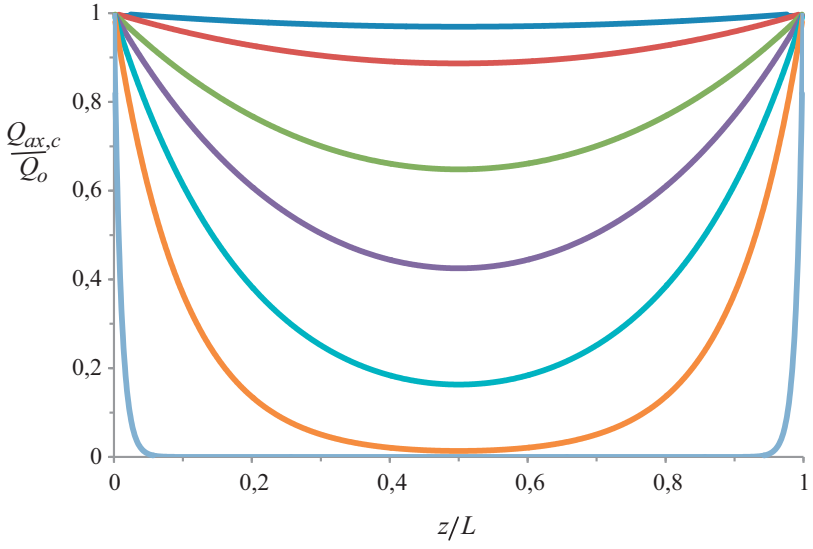

Fig. 2. Relative flow rate in the channel, $Q_{ax,c}/Q_o$, vs. relative position, z/L, along the channel, according to Eq. (14). From upper to lower curves: $\rho = 0.5, 1, 2, 3, 5, 10, 100$.

the porous element), one has:

$$Q_{ax,c} + Q_{ax,r} = Q_o \tag{5}$$

hence:

$$\frac{dQ_{ax,c}}{dz} + \frac{dQ_{ax,r}}{dz} = 0 \tag{6}$$

where $Q_{ax,r}$ is the flow rate at position z in the reservoir, Q_o is the flow rate at the channel inlet (and outlet). The part of the flow entering the slice dz in the channel which is not exiting this slice in the channel is necessarily flowing through the porous element, perpendicularly to axis z, within which the Darcy law applies. Hence:

$$-\frac{dQ_{ax,c}}{dz} = \frac{k}{\eta}\frac{P_c(z) - P_r}{h} \tag{7}$$

Getting the derivative of Eq. (7) with respect to z gives:

$$-\frac{d^2Q_{ax,c}}{dz^2} = \frac{k}{\eta h}\frac{dP_c}{dz} \tag{8}$$

Elimination of dP_c/dz between Eqs. (4) and (8) gives the basic differential equation for the channel flow rate:

$$\frac{d^2Q_{ax,c}}{dz^2} = \frac{12k}{w^3h}Q_{ax,c} = \frac{Q_{ax,c}}{\Lambda^2} \tag{9}$$

where Λ is a characteristic length:

$$\Lambda = \sqrt{\frac{w^3h}{12k}} \tag{10}$$

This characteristic length is essentially the same as that described by Déjardin in his model for asymmetrical flow FFF with a semi-permeable membrane having a permeability gradient [15], except that here, it pertains to the porous element and we assume that the permeability of the porous element is uniform.

It can be verified that a general solution to Eq. (9) is:

$$Q_{ax,c} = A\,\exp(z/\Lambda) + B\,\exp(z/\Lambda) \tag{11}$$

where A and B are integration constants.

2.1.2. Flow rate profile in the channel

Eq. (11) can be solved using the limiting conditions of the problem. At the inlet and outlet of the channel, we have: $Q_{ax,c}(z=0) = Q_{ax,c}(z=L) = Q_o$. Applying these two conditions to Eq. (11) allows to eliminate the constants A and B, which gives the flow rate profile along the channel:

$$\frac{Q_{ax,c}(z)}{Q_o} = \frac{\sinh(z/\Lambda) + \sinh((L-z)/\Lambda)}{\sinh(L/\Lambda)} \tag{12}$$

Defining ρ as:

$$\rho \equiv \frac{L}{\Lambda} = \sqrt{\frac{12kL^2}{w^3h}} \tag{13}$$

Eq. (12) can be written as:

$$\frac{Q_{ax,c}(z)}{Q_o} = \frac{\sinh(\rho(z/L)) + \sinh(\rho(1-(z/L)))}{\sinh\,\rho} \tag{14}$$

Eq. (14) indicates that the flow rate profile in the channel is symmetrical with regard to the position $z/L = 1/2$, for which the channel flow rate has its minimum value equal to:

$$\frac{Q_{ax,c}(z=L/2)}{Q_o} = \frac{2\,\sinh(\rho/2)}{\sinh\,\rho} \tag{15}$$

Λ and ρ appear to be the relevant parameters in this problem.

2.1.3. Pressure drop and pressure gradient profile

If the two channel walls were impermeable, the pressure drop between the channel inlet and outlet would be ΔP_0 equal to (for an infinite parallel wall configuration):

$$\Delta P_0 = \frac{12\eta Q_o L}{w^3} \tag{16}$$

(Note that this equation is dimensionally correct because Q_o is a flow rate per unit breadth).

From Eq. (7), one gets:

$$P_c(z/L) - P_r = -\frac{\eta h}{k}\frac{dQ_{ax,c}}{dz} = -\frac{\eta h Q_o}{kL}\frac{d(Q_{ax,c}/Q_o)}{d(z/L)} \tag{17}$$

which gives after derivation of Eq. (14) with respect to z/L:

$$P_c(z/L) - P_r = -\frac{\eta h Q_o}{kL}\frac{\rho[\cosh(\rho(z/L)) - \cosh(\rho(1-(z/L)))]}{\sinh\,\rho} \tag{18}$$

It is seen that, since the flow rate profile is symmetrical relative to $z/L = 1/2$, its derivative at this point is zero and, according to Eq. (17), the pressure in the channel at this point is equal to the pressure of the reservoir. This means that, at the middle of the channel, the liquid ceases to flow from the channel to the reservoir but, instead, as one goes from this position toward the channel outlet, liquid starts to flow from the reservoir back to the channel. Applying Eq. (18) for $z/L = 0$ and $z/L = 1$ and combining resulting equations with Eq. (13) to eliminate P_r, one gets the pressure drop, $P_i - P_o$:

$$\frac{P_i - P_o}{\Delta P_0} = \frac{2(\cosh\,\rho - 1)}{\rho\,\sinh\,\rho} \tag{19}$$

Noting that: $P_i - P_o = 2(P_r - P_o)$, one gets the relative pressure profile from Eqs. (18) and (19):

$$\frac{P_c(z/L) - P_o}{P_i - P_o} = \frac{\cosh(\rho(1-(z/L))) - \cosh(\rho(z/L))}{2(\cosh\,\rho - 1)} + \frac{1}{2} \tag{20}$$

2.2. A single permeable wall with frit and membrane (asymmetrical flow FFF)

The porous element of an asymmetrical flow FFF channel is made of a frit of permeability k_f and height w_f backing a semi-permeable membrane of permeability k_m and thickness w_m. The membrane and frit constitute then two resistances to transversal flow in series. In an infinitesimal slice of the system assembly, since there is no accumulation of liquid in the system, the transversal velocity, u_{tr}, in the membrane is equal to that in the frit. If $P_{int}(z)$ is the pressure at the interface between the membrane and the frit, when applying Darcy law to the transversal flow in the membrane and in the frit, we have, for the membrane:

$$u_{tr}(z) = \frac{k_m}{\eta w_m}[P_c(z) - P_{\mathrm{int}}(z)] \tag{21}$$

and for the frit:

$$u_{tr}(z) = \frac{k_f}{\eta w_f}[P_{\mathrm{int}}(z) - P_r(z)] \tag{22}$$

For the sake of consistency, all permeabilities used in this study have the dimension of the square of a length as can be checked in Eqs. (21) and (22), since they are defined, according to Darcy law, as velocity (distance travelled per unit time) per unit pressure gradient for a fluid of unit viscosity. Noting that $u_{tr} = -dQ_{ax,c}(z)/dz$, and eliminating $P_{int}(z)$ between Eqs. (21) and (22), we get:

$$-\frac{dQ_{ax,c}(z)}{dz} = \frac{P_c(z) - P_r}{\eta((w_m/k_m) + (w_f/k_f))} \tag{23}$$

Comparing Eqs. (7) and (23) shows that a system with a membrane and a frit is equivalent to a system with one porous element for

which the effective permeability, k_{eff}, and height, h_{eff}, are such that:

$$\frac{h_{eff}}{k_{eff}} = \frac{w_m}{k_m} + \frac{w_f}{k_f} \tag{24}$$

For such a system, the flow rate and pressure profile along the channel are still given by Eqs. (14) and (20), with the characteristic length Λ still given by Eq. (10) in which h/k is replaced by h_{eff}/k_{eff}. Then, the pressure P_{int} is such that:

$$\frac{P_{\text{int}}(z) - P_r}{P_c(z) - P_r} = \frac{w_f/k_f}{(w_m/k_m) + (w_f/k_f)} \tag{25}$$

This pressure ratio does not depend on the position z.

2.3. Two permeable walls (symmetrical flow FFF)

Let us now consider the system depicted in Fig. 1B for which each side wall is permeable and made of a porous element. The permeabilities and heights of the porous elements are, respectively, k_1 and h_1 for wall 1, k_2 and h_2 for wall 2. These quantities are effective quantities, as described in the above section, for the accumulation wall side made of a membrane/frit assembly. Behind each porous element is a reservoir where the pressure, assumed constant all along the system, is P_{r1} for side 1, P_{r2} for side 2.

Eq. (4) still describes the flow rate in the channel. Let $Q_{ax,r1}$ and $Q_{ax,r2}$ be the axial flow rates in reservoirs 1 and 2, respectively. The variation of $Q_{ax,r1}$ in slice dz is equal to the transversal flow rate through the porous element 1 in this slice. This is also true for porous element 2 and reservoir 2. One then has, from Darcy law:

$$\frac{dQ_{ax,r1}}{dz} = \frac{k_1}{\eta}\frac{P_c(z) - P_{r1}}{h_1} \tag{26}$$

and:

$$\frac{dQ_{ax,r2}}{dz} = \frac{k_2}{\eta}\frac{P_c(z) - P_{r2}}{h_2} \tag{27}$$

Flow rate conservation gives:

$$Q_o = Q_{ax,c} + Q_{ax,r1} + Q_{ax,r2} \tag{28}$$

hence:

$$\frac{dQ_{ax,c}}{dz} + \frac{dQ_{ax,r1}}{dz} + \frac{dQ_{ax,r2}}{dz} = 0 \tag{29}$$

After derivation and combination of Eqs. (4) and (26)–(29), one gets:

$$\frac{d^2Q_{ax,c}}{dz^2} = \frac{12}{w^3}\left(\frac{k_1}{h_1} + \frac{k_2}{h_2}\right)Q_{ax,c} \tag{30}$$

This differential equation is similar to Eq. (9) except that one has now:

$$\Lambda = \sqrt{\frac{w^3}{12((k_1/h_1) + (k_2/h_2))}} \tag{31}$$

Therefore, the flow rate and pressure profile in the channel itself are still given by Eqs. (14) and (20), respectively. They depend on the sole parameter $\rho = L/\Lambda$ with Λ given by Eq. (31). One notes that if the values of k/h are the same for the two porous elements, the result is equivalent to that of a single porous element with half its initial height. If now the second porous element is such that $k_2/h_2 \ll k_1/h_1$, it behaves as a solid wall.

2.4. Physical meaning of Λ

The physical meaning of Λ was described by Déjardin as the length of a channel with one porous element having the same hydraulic resistance as the porous element (see Fig. 1 of [16]). An alternative physical meaning can be derived from the flow equations derived in Section 2.1. Eq. (14) shows that, because the carrier liquid can flow through a permeable wall, the flow rate within the channel itself decreases from the inlet to the middle of the channel. The relative rate of decrease of the channel flow rate with distance, at the channel inlet, is obtained from Eq. (14) as:

$$-\frac{dQ_{ax,c}(z=0)/Q_o}{d(z/L)} = \frac{\rho(1 - \cosh\,\rho)}{\sinh\,\rho} \tag{32}$$

It can be shown that this rate of flow decrease becomes equal to ρ as ρ increases. The error in this approximation is less than 10% for $\rho = 3$ and is only 1.3% for $\rho = 5$. This implies that the slope at the origin of the plot of $Q_{ax,c}/Q_o$ vs. z/L hits the z/L axis at $1/\rho$. Hence, for systems with relatively large ρ values, the characteristic length Λ appears to be that characteristic distance over which occurs most of the flow rate variation along the channel.

2.5. Residence time in the channel

Because the flow in the channel is lower than if there was no flow through the porous element, the residence time in the channel of a species used to probe the channel void volume, in this no-field case, is larger than expected. Two cases can be considered for this probe. First, it can be a low molar mass solute which samples all the carrier flow streamlines. A fraction of the solute can then leave the channel through the frit and the reservoir. This fraction can be considered as lost. In fact, it can reenter the channel in its second half. But it will then be so diluted that it can hardly be detected. The second case is that of a colloidal species which is too big to leave the channel through the pores of the porous element, but at the same time is small enough for sampling all the flow streamlines in the channel, i.e. it does not undergo steric exclusion from the channel wall or hydrodynamic lift forces (in practice, these conditions may not be compatible). In both cases, if a small amount of tracer is injected in the channel, the mean residence time, t_o, of the fraction of the tracer which remains in the channel is:

$$t_o = \int_0^L \frac{dz}{u_c(z)} = w\int_0^L \frac{dz}{Q_{ax,c}(z)} \tag{33}$$

where $u_c(z)$ is the cross-sectional average carrier velocity in the channel at location z and $Q_{ax,c}(z)$ is given by Eq. (14). This residence time can be compared to the classical residence obtained, for the same inlet flow rate Q_o, in a channel of the same geometry with plain walls, $t_{oo} = wL/Q_o$:

$$\frac{t_o}{t_{oo}} = \sinh\,\rho\int_0^1 \frac{dx}{\sinh\,\rho x + \sinh\,\rho(1-x)} \tag{34}$$

which gives, after integration:

$$\frac{t_o}{t_{oo}} = \frac{4e^{\rho/2}\,\sinh\,\rho}{\rho(e^{\rho} - 1)}\left[\arctan(e^{\rho/2}) - \frac{\pi}{4}\right] \tag{35}$$

This time ratio depends on the sole parameter ρ and is independent on actual flow rate. Hence, doubling the flow rate will result in decreasing by a factor 2 the residence time even if it differs significantly from the time expected for a channel with solid walls. This is a consequence of the linearity of the flow equations used in the Stokes regime (Poiseuille flow in the channel, Darcy flow though the porous elements).

The above equations for the flow and pressure profiles as well as for the residence time are valid for both symmetrical and asymmetrical flow FFF provided the appropriate ρ value is used. It should however be noted that they are obtained with the assumption of a constant channel breadth. They are therefore not applicable to asymmetrical flow FFF channels with trapezoidal shape [17] or with exponentially decreasing breadth [18]. Such specific geometries can be taken into account in the flow equations. It can be expected that the results will then be numerically different but

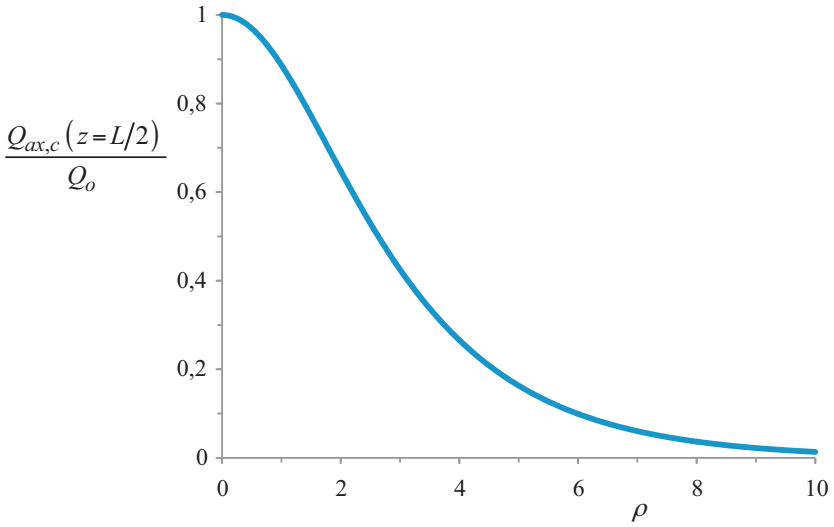

Fig. 3. Relative flow rate in the channel, $Q_{ax,c}/Q_o$, at the mid-length of the channel ($z = L/2$) vs. ρ, according to Eq. (15).

their features will be essentially similar to those presented here, as they reflect the essential fact that the carrier liquid can bypass the channel depending on the actual value of ρ.

In addition, for the calculation of the residence time, it is assumed that the analyte starts its migration in the channel from $z = 0$ (see the lower limit of integration in Eq. (33)). If the starting position were different (as it is frequently the case in asymmetrical flow FFF due to the sample focusing procedure), Eqs. (33)–(35) have to be accordingly modified. It is likely that the resulting t_o/t_{oo} will be larger than for an analyte starting from $z = 0$, since at the starting position, the channel flow rate will be lower than at the inlet.

3. Experimental

3.1. Flow FFF experiments

A home-made symmetrical flow FFF with length $L = 41$ cm (tip to tip) and breadth $b = 1.5$ cm was designed according to literature description [19]. The Mylar spacer was 260 μm thick. The calculated geometrical volume, V_g, of the channel was 1.52 mL. The porous walls consisted of 2.5 mm thick stainless steel plates backed by 6 mm thick polyethylene plates. One of the walls was covered by a semi-permeable membrane (PH 79 nitrocellulose membrane with 0.1 μm pore size, gift from Schleicher & Schuell, Dassel, Germany, now membrane NC 10 available from Whatman, Maidstone, UK). Polystyrene latex particles of 0.45 μm (Estapor, Prolabo, Paris, France) were injected. The particles were dispersed in the carrier liquid (water solution containing 0.3% sodium dodecyl sulfate and 0.02% sodium azide). A liquid chromatographic pump (Model 114, Beckman, San Ramon, USA) was used for carrier delivery and the elution of the particles was recorded by a UV photometer (Model 440, Waters, Milford, USA).

3.2. Frit permeability measurements

For the determination of the permeability of a frit, a circular piece of frit of diameter 1.0 cm was cut and sealed inside a frit holder, so that the liquid flowing through the holder was forced to flow through the frit. The holder was positioned horizontally and water was pumped by means of the LC pump inside the frit holder from below. A Teflon tube was connected by means of a Swagelok tee to the tube connecting the pump to the frit holder. The other end of the Teflon tube was connected to the bottom of a vertical burette. The difference in steady state height of water in the burette obtained when the pump was turned on then off allowed the determination of the frit permeability, knowing the flow rate, density and viscosity of water. The experiment was repeated without frit in the holder in order to subtract the contribution of the connecting lines to the flow resistance of the system. The permeabilities of the stainless steel and polyethylene frits were found equal to 0.91×10^{-8} cm^2 and 1.92×10^{-8} cm^2, respectively. The values of the permeability and thickness of the membrane were provided by the manufacturer and equal to 9.72×10^{-12} cm^2 and 105 μm, respectively.

4. Results and discussion

Fig. 2 shows the flow rate profiles, $Q_{ax,c}(z/L)/Q_o$ vs. z/L, given by Eq. (14), obtained when closing the transversal inlet and outlet flow lines, for various ρ values. This figure applies to both asymmetrical and symmetrical flow FFF channels since both types of channels are characterized by a value of ρ. This illustrates that, because the liquid encounters a relatively large flow resistance in the thin and long channel, part of this liquid is deflected to the reservoir(s) near the channel inlet, flows along the reservoir(s) and returns to the channel near the channel outlet. That fraction of the carrier flow rate which flows along the reservoir(s) is the complement to 1 of the curves of Fig. 2. It is clear that the larger ρ, the bigger the deviation from the ideal situation in which $Q_{ax,c}$ is constant and equal to Q_o for any z, hence the bigger the relative flow in the reservoir(s). Eq. (13) indicates that the longer and thinner is the channel, and the more permeable and thin are the permeable elements of the porous walls, the larger the flow in the reservoir(s).

The minimum flow rate in the channel is observed at mid-channel length. At this point, the liquid ceases to flow transversally from the channel to the reservoir(s) and starts to flow from the reservoir(s) back to the channel. This minimum relative flow rate, given by Eq. (15), at the middle of the channel, is shown vs. ρ in Fig. 3.

The relative pressure profile in the channel is plotted for different ρ values in Fig. 4. In the case of a channel with impermeable walls, ρ is equal to zero and the pressure profile is linear. It is seen from Fig. 4 that the deviation from the linearity increases with increasing ρ. It is also interesting to compare $P_c(z) - P_o$, not to the actual pressure drop $P_i - P_o$, but to the hypothetic pressure drop that would be obtained for the same flow rate Q_o in a channel with

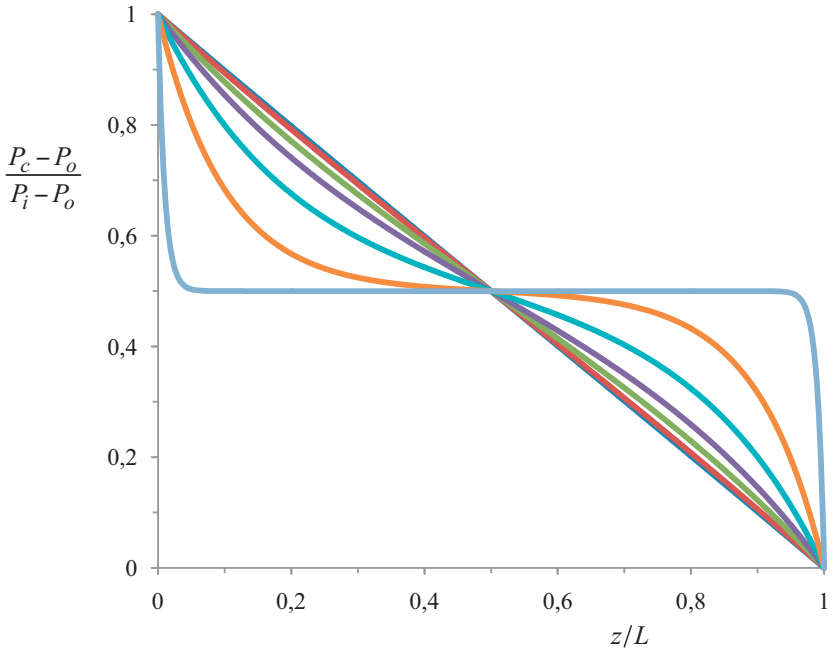

Fig. 4. Relative pressure profile in the channel, $(P_c - P_o)/(P_i - P_o)$, according to Eq. (20), for various ρ values. From upper to lower curves for $z/L < 1/2$: $\rho = 0, 0.5, 1, 2, 3, 5, 10$.

solid walls, ΔP_0. The corresponding curves are plotted in Fig. 5. These curves are similar in shape to those of Fig. 4, but it seen that the actual pressure at any point in the channel is lower than for a channel with solid walls, the more so as ρ is larger. This reflects the fact that the liquid encounters less resistance to flow to the outlet when it can find its way through the frit(s) and the reservoir(s) than when the walls are impermeable.

In Fig. 6, the elution time, t_o, of a species relative to the time, t_{oo}, one would expect from Eq. (3) on the basis of the channel volume, V_g, and the measured flow rate, F_o, is plotted as a function of ρ. The three plots correspond to Eq. (35) and are given for three different ρ ranges. It is seen that, for ρ values exceeding a few units, the tracer residence time may be much larger than expected. Furthermore, it is seen to increase very fast with increasing ρ.

Experiments have been performed by injecting 0.45 μm polystyrene latex particles in the flow FFF system described in the previous section, with the inlet and outlet transversal lines closed. They were repeated several times at two different flow rates, F_o (where F_o is the volume of carrier flowing in or out of the channel per unit time, i.e. $F_o = bQ_o$). The residence times, t_o, of the particles were measured. Whatever the flow rate, the ratio t_oF_o/V_g was found constant, within experimental uncertainties, and equal to 15.6. This ratio is equal to the ratio of the measured elution volume to the geometrical channel volume. It should correspond to t_o/t_{oo}. This result shows clearly that, for the flow FFF system used, the no-field method leads to a very large error for the determination of the void time or void volume. This comes from the fact that, in this approach, the length-averaged flow rate in the channel itself is

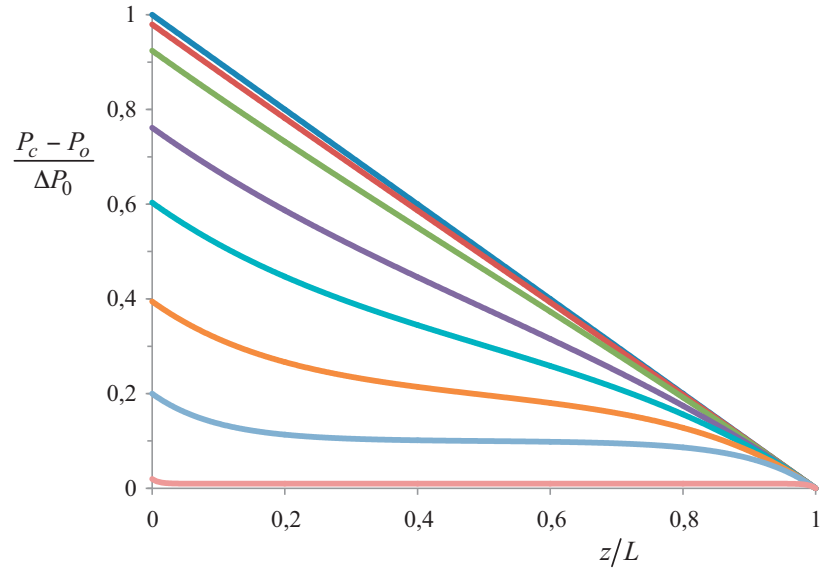

Fig. 5. Pressure profile, $P_c - P_o$, in the channel, relative to the hypothetic pressure drop, ΔP_o, that would be obtained, for the same inlet flow rate, if the channel walls were impermeable. From upper to lower curves: $\rho = 0, 0.5, 1, 2, 3, 5, 10, 100$.

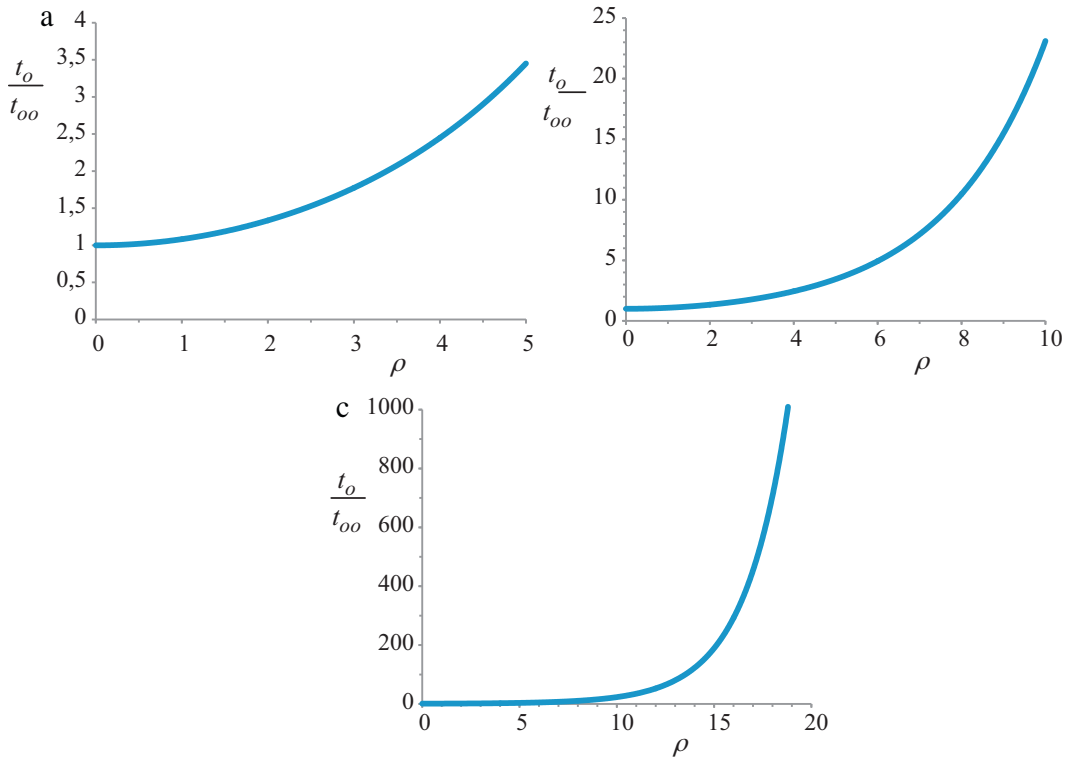

Fig. 6. Elution time, t_o, relative to the hypothetic elution time that would be obtained, for the same inlet flow rate, if the channel walls were impermeable, t_{oo}, vs. ρ. (A) ρ range: 0–5; (B) ρ range: 0–10; (C) ρ range: 0–20.

only 1/15.6, i.e. 6.4% only of the total flow rate. Hence, in average, 93.6% of the inlet flow rate is bypassing the channel and flows from the channel to the outlet through the reservoirs of the system.

Eq. (35) indicates that this t_o/t_{oo} value corresponds to a ρ value equal to 9.02. We can compare this value with the expression given by the ρ expression in Eq. (13). Taking $L = 41$ cm and $w = 260$ μm, this gives a ratio k_{eff}/h_{eff} equal to 7.09×10^{-8} cm. It would be interesting to compare this value with that calculated from the measured permeabilities of the wall elements. The effective k/h value for the depletion wall, $(k/h)_d$, can be calculated using Eq. (24) for two porous elements in series (they can be the membrane and a frit in series or the two frits in series). From the measured permeabilities of these frits, this gives $(k/h)_d = 1.70 \times 10^{-8}$ cm. Similarly, extending the additivity law of Eq. (24) to three permeable elements (membrane, metal frit and polyethylene frit), we found that, for the accumulation wall, $(k/h)_a = 8.78 \times 10^{-10}$ cm. As expected, because of the presence of the semi-permeable membrane, the accumulation wall is much less permeable than the depletion wall. Then, using Eq. (31), the effective k/h of the flow FFF system with two porous walls, $(k/h)_{eff}$, is found equal to 1.79×10^{-8} cm. This is quite smaller than the value derived from t_o/t_{oo}. It should however be noted that the value of t_o/t_{oo} was derived using the geometrical volume of the channel on the basis of the nominal value of the spacer thickness, $w_{nom} = 260$ μm. In fact, it is likely that the membrane protrudes inside the channel, hence reducing its thickness to an effective value, w_{eff}. Then, the effective t_o/t_{oo} value should be equal to that based on the nominal geometrical volume, multiplied by w_{nom}/w_{eff}. In addition, the value of ρ should, according to Eq. (13), be multiplied by $(w_{nom}/w_{eff})^{3/2}$. Doing these transformations, we find that the effective channel thickness that would give the experimentally observed elution time for the particles, according to Eq. (35) is equal to 150 μm. Then, the effective value of t_o/t_{oo} is 27.1, and the corresponding ρ value is 10.4. This thickness value corresponds to a rather significant protrusion of the membrane inside the channel (42% reduction of channel thickness). Comparable values for channel reduction due to membrane protrusion have been reported [20].

Although there are some uncertainties in the values of some experimental parameters, especially those related to the permeabilities of the porous elements and to the effective channel thickness, the above calculations show that the much larger than expected elution time of particles in absence of cross-flow is well accounted for by the model developed in the theory section.

This study shows that the permeability characteristics of the porous elements play a significant role in the flow behavior in the flow FFF channels. They are usually not reported and, often, not known. Still, the k/h values of some porous ceramic frits specifically developed for flow FFF have been reported by Dean et al. [21]. Their A to E frits had k/h values of 6.2×10^{-8} cm, 9.7×10^{-7} cm, 1.8×10^{-6} cm, 1.5×10^{-8} cm and 3.3×10^{-7} cm, respectively. Except frit D, they are more permeable than the frit system used in our study. Hence, they are more prone to liquid flow bypass to the reservoir(s). For a 30 cm long channel with a thickness of 254 μm, this corresponds to ρ values of 6.4, 25.3, 34.4, 3.1, 14.7, respectively and to t_o/t_{oo} values of 5.7, 1.9×10^4, 1.4×10^6, 1.8 and 170, respectively.

The peak of the detected tracer particles is much lower than it would be for a channel with impervious walls. Since the particles flowing through the frit with the carrier are considered to be lost, the fraction of the particles remaining within the channel, i.e. the fraction of the particles detected, is equal to the ratio of the lowest flow rate in the channel to the inlet flow rate, i.e. $Q_{ax,c}(z/L = 1/2)/Q_o$, which is plotted vs. ρ in Fig. 3. For the two situations corresponding to our experiments, that fraction amounts to 1.1%.

5. Conclusion

The experimental determination of the elution time of colloidal particles in absence of cross-flow was found much larger than expected on the basis of the nominal value of the geometrical

volume of the channel. In spite of uncertainties in the precise value of the effective permeability of the permeable elements of the flow FFF system used, this result comforts the flow model described in the theory section. This model allows the carrier liquid to leave the channel itself for reaching the reservoir(s) by flowing through the porous wall(s) in the first part of the channel, flow along the reservoir(s) and return to the channel by flowing again through the porous wall(s) from the reservoir(s) to the channel before the channel outlet. In our system, the reservoir(s) flow rate was quite significant.

This approach for elution time determination is called the "no-field method" because it corresponds to the absence of a net cross-flow. However, the analysis developed in this study reveals that it should be renamed "average no-field method" because it may indeed hide strong local fields (cross-flow) compensating each other along the channel length.

From Eq. (35), the conditions to be fulfilled for the no-field method of void time determination to be satisfying can be obtained by noting that:

$$\lim_{\rho\to 0}\frac{t_o}{t_{oo}} = 1 + \frac{\rho^2}{12} + O(\rho^6) \tag{36}$$

Combining this limit with Eq. (13) shows that in order to allow the determination of t_o by the no-field method with a tolerated error smaller than ε (e.g., 1%), the effective k/h value for the permeable elements of the channel must be such that:

$$\left(\frac{k}{h}\right)_{eff} \leq \varepsilon\frac{w^3}{L^2} \tag{37}$$

For this condition to be satisfied in the case of our channel, $(k/h)_{eff}$ should have been smaller than about 10^{-10} cm, which was not the case. The characteristics of the ceramic frits developed for flow FFF by Dean et al. are very unlikely to fulfill condition (37), unless short and thick channels are used, but, then, the resolution of the separation will be impaired.

These considerations show that the no-field method for void time and volume determination must be prohibited for flow FFF. Instead the rapid breakthrough method developed by Giddings et al. [9] should be used.

Anyway, the full understanding of the liquid flow behavior in symmetrical or asymmetrical flow FFF channels requires the knowledge of the effective permeability and thickness of the permeable wall elements. It is desirable that these data are given by manufacturers of flow FFF instruments. If the no-field method for t_o determination must be rejected in flow FFF, at least in their present-day configuration, the present study illustrates that the liquid in any part of the system tends to flow where it encounters the least hydrodynamic resistance. This basic behavior also occurs when a cross-flow is applied. The knowledge of the frit characteristics would be much helpful for studying the complete flow pattern in symmetrical or asymmetrical flow FFF with cross-flow, in order to determine the extent of deviation from the usual ideal model where the cross-flow velocity is constant all along the channel, at least, in the vicinity of the accumulation wall.

Acknowledgements

Fruitful discussions with Jean-Pierre Hulin and E. John Hinch, as well as the experimental assistance of Xiaoqin Chen for the residence time measurements are gratefully acknowledged.

References

[1] J.C. Giddings, J. Chem. Educ. 50 (1973) 667.
[2] M. Martin, J. High Resolut. Chromatogr. (HRC) 19 (1996) 481.
[3] M.E. Hovingh, G.H. Thompson, J.C. Giddings, Anal. Chem. 42 (1970) 195.
[4] M. Martin, S. Garcia-Martin, M. Hoyos, J. Chromatogr. A 960 (2002) 165.
[5] K.-G. Wahlund, J.C. Giddings, Anal. Chem. 59 (1987) 1332.
[6] J.C. Giddings, G.-C. Lin, M.N. Myers, J. Liq. Chromatogr. 1 (1978) 1.
[7] A. Litzén, K.-G. Wahlund, J. Chromatogr. 476 (1989) 413.
[8] J.C. Giddings, F.J. Yang, M.N. Myers, Anal. Biochem. 81 (1977) 395.
[9] J.C. Giddings, P.S. Williams, M.A. Benincasa, J. Chromatogr. 627 (1992) 23.
[10] M.K. Liu, P.S. Williams, M.N. Myers, J.C. Giddings, Anal. Chem. 63 (1991) 2115.
[11] M.H. Moon, J.C. Giddings, J. Pharm. Biomed. Anal. 11 (1993) 911.
[12] M.-K. Liu, P. Li, J.C. Giddings, Protein Sci. 2 (1993) 1520.
[13] A.M. Botana, S.K. Ratanathanawongs, J.C. Giddings, J. Microcol. Sep. 7 (1995) 395.
[14] S.K.R. Williams, in: M. Schimpf, K. Caldwell, J.C. Giddings (Eds.), Field-Flow Fractionation Handbook, Wiley-Interscience, New York, 2000, p. 257 (Chapter 17).
[15] P. Déjardin, J. Chromatogr. A 1187 (2008) 209.
[16] P. Déjardin, J. Chromatogr. A 1203 (2008) 94.
[17] A. Litzén, K.-G. Wahlund, Anal. Chem. 63 (1991) 1001.
[18] P.S. Williams, J. Microcol. Sep. 9 (1997) 459.
[19] J.C. Giddings, M.N. Myers, K.D. Caldwell, S.R. Fisher, in: D. Glick (Ed.), Methods of Biochemical Analysis, vol. 26, Wiley, New York, 1980, p. 79.
[20] C. Contado, A. Dalpiaz, E. Leo, M. Zborowski, P.S. Williams, J. Chromatogr. A 1157 (2007) 321.
[21] G.A. Dean, C.M. Cardile, R.J. Steal, I.D. Alecu, J. Mater. Sci. Lett. 13 (1994) 872.

Glossary of symbols

A: integration constant in Eq. (11)
B: integration constant in Eq. (11)
b: channel breadth
b_r: breadth of the reservoir
F: force exerted by the external field on an analyte molecule or particle
F_o: carrier flow rate measured at the channel outlet
h: height of a porous element (frit or membrane)
h_{eff}: effective height of a frit and membrane assembly
k: permeability of a porous element (frit or membrane)
k_{eff}: effective permeability for a membrane and frit assembly
k_f: permeability of the porous frit
k_m: permeability of the semi-permeable membrane
L: channel length
P_c: pressure in the channel
P_i: pressure at channel inlet
P_{int}: pressure at the interface between the membrane and the frit
P_o: pressure at channel outlet
ΔP_0: hypothetic channel pressure drop that would be obtained for the same carrier flow rate if the channel walls were impermeable
P_r: pressure in the reservoir
$Q_{ax,c}$: axial carrier flow rate per unit breadth in the channel
$Q_{ax,r}$: axial carrier flow rate in the reservoir per unit channel breadth
Q_o: carrier flow rate at channel inlet (or outlet) per unit channel breadth
R: retention ratio
S_c: cross-sectional surface area of the channel
t_o: void time
t_{oo}: hypothetic void time that would be obtained for the same carrier flow rate if the channel walls were impermeable
t_R: analyte retention time
u_c: cross-sectional average carrier velocity in the channel
u_{tr}: transversal carrier flow velocity
$\langle v\rangle$: mean flow linear velocity
$\mathcal{V}$: analyte advection velocity
V_g: geometrical volume of the channel
V_o: void volume
V_R: analyte retention volume
w: channel thickness
w_{eff}: effective channel thickness
w_f: thickness (height) of the porous frit
w_m: thickness of the semi-permeable membrane
w_{nom}: nominal value of the channel thickness
w_r: thickness (height) of the reservoir
z: distance along the channel from inlet
η: dynamic viscosity of the carrier liquid
Λ: characteristic length defined by Eq. (10)
ρ: ratio of channel length to characteristic length Λ